Infrared to visible up-conversion study for erbium-doped zinc tellurite glasses

2000 J. Phys.: Condens. Matter 12 4523

(http://iopscience.iop.org/0953-8984/12/20/307)

J. Phys.: Condens. Matter **12** (2000) 4523–4534. Printed in the UK PII: S0953-8984(00)10894-X

Infrared to visible up-conversion study for erbium-doped zinc tellurite glasses

N Jaba, A Kanoun, H Mejri, A Selmi, S Alaya and H Maaref

Laboratoire de Physique des Semiconducteurs, Département de Physique, Faculté des Sciences, 5019, Monastir, Tunisia

E-mail: hassen.maaref@fsm.rnu.tn

Received 11 January 2000

Abstract. Optical absorption and photoluminescence properties of Er^{3+}-doped $70TeO_2$–$30ZnO$ glass are investigated. Judd–Ofelt intensity parameters of Er^{3+} have been determined to calculate the radiative transition probabilities and the radiative lifetimes of excited states. An infrared to visible up-conversion was observed at room temperature in this tellurite glass system using a 797 nm excitation line. A study of the $^4S_{3/2}$–$^4I_{15/2}$ transition (554 nm) versus power excitation provided evidence for a two-step up-conversion process under this excitation. A red emission (663 nm) originating from the $^4F_{9/2}$–$^4I_{15/2}$ transition has been observed as well. It was found that the efficiency of this up-conversion line is enhanced considerably with the Er^{3+} concentration relative to the green emission (554 nm). This behaviour has been explained in terms of an energy transfer between excited ions. The temperature dependence of up-conversion intensity has been also studied in the range 40–310 K. It was found that the thermal quenching of the green emission ($^4S_{3/2}$–$^4I_{15/2}$) is large enough compared with those of the red transition ($^4F_{9/2}$–$^4I_{15/2}$). This thermal quenching has been discussed using the Riseberg and Moos model of multiphonon emission. It has been shown that the latter approach is not consistent with existing results. A complete analysis of the temperature-dependent up-conversion has been made using an additional decay rate which may be attributed to a non-radiative energy transfer and/or a charge transfer through trapping impurities. A good agreement has been achieved between measured and computed data.

1. Introduction

Extensive studies have been made on the conversion of long-wave light to shorter wavelength radiations in rare-earth (RE)-doped materials [1–8]. Up-conversion has stimulated interest in the development of optical devices such as visible laser sources pumped by an infrared line excitation [9–11], optical fibres [12], sensors and under-sea optical communications [7]. The opposite to solids, glasses are attractive due to the fact that large quantities of RE ions can be incorporated in these host lattices [13], and also they present the advantage that they can be used in optical fibre technology. However, the up-conversion efficiency is influenced by the ligand field, the multiphonon relaxation processes and optical properties of the host material [9]. Thus, the glassy host is required to posses a minimal absorption coefficient within the wavelength of interest and the capability of incorporating high RE concentrations, low vibrational phonon energies and a high refractive index. Fluoride crystals and glasses are the most studied hosts because of their lower vibrational energies [8, 14–16]. Germanate- and tellurite-based oxide glasses generally have better mechanical strength, chemical durability and thermal stability than fluoride-based glasses [12]. In addition, tellurite glasses have the lowest maximum phonon energy among oxide glasses and a larger refractive index, both of

0953-8984/00/204523+12$30.00

which are beneficial for radiative transitions of RE ions [12, 17, 18]. Therefore, these hosts are suitable for up-conversion luminescence. Er^{3+} is the most commonly used RE dopant that can provide up-converted visible fluorescence both in fluoride crystals and glasses [9, 10, 14] and in oxide glasses [4, 19].

In this paper we report the effects of Er^{3+} ion concentration and temperature on the up-conversion processes in zinc tellurite glass excited with 797 nm near-infrared line. The samples are doped with different Er_2O_3 concentrations ranging from 0.2 to 4 mol.%. Optical absorption and emission for different levels have been measured and analysed using the Judd–Ofelt theory. Up-converted green emission $^4S_{3/2}$–$^4I_{15/2}$ was observed at room temperature in this glass host independent of the Er^{3+} content. A red transition of $^4F_{9/2}$–$^4I_{15/2}$ has been also detected. This emission shows rapid growth relative to the green up-converted line as the Er^{3+} concentration increases. Possible up-conversion mechanisms have been used to explain the behaviour of the latter transition. From the temperature dependence studies, it was revealed that the green up-converted line shows a thermal quenching. The red emission does not, however, exhibit a significant change as temperature varies. An analysis has been made for the quenching behaviour of the $^4S_{3/2}$–$^4I_{15/2}$ transition: (i) using the Riseberg and Moos model of multiphonon emission, (ii) with the adjunction of another non-radiative transition rate. An attempt to explain all these results will be presented.

2. Experimental

Glasses were prepared from oxide powders of TeO_2, ZnO and Er_2O_3 as starting materials using the conventional melt-quenching method. The amount of dopant was varied between 0.2 and 4 mol.% Er_2O_3. The visible and near-infrared absorption spectra were measured at room temperature using a Shimadzu UV 1201 spectrophotometer in the 370–1000 nm range. Photoluminescence (PL) spectra were recorded by exciting the samples with 488 nm light from a cw argon laser Spectra-physics 2017. A cw near-infrared Ti:saphire laser tuned to 797 nm was used for up-conversion excitation. The emitted light was dispersed by a Jobin–Yvon HRD1 monochromator and detected with a Hamamatsu R 943-02 photomultiplier. The signal from the detector was preamplified and passed to a lock-in amplifier whose reference was a variable speed light chopper in the excitation beam. The samples were mounted in a helium cryostat for temperature-dependent studies in the range 10–310 K.

3. Absorption and photoluminescence data—Judd–Ofelt analysis

Visible and near-infrared measurements were performed on a series of Er^{3+}-doped $70TeO_2$–30ZnO glasses at room temperature. Figure 1 shows the typical absorption spectrum of the sample containing 1 mol.% Er_2O_3. The absorption lines were recorded relative to the undoped sample, and are therefore reported as the absorption coefficient of Er^{3+} in the host glass. We give in the same figure the electronic transitions assigned to the absorption bands, the ground state is the $^4I_{15/2}$ level. Luminescence originating from the excited $^2H_{11/2}$, $^4S_{3/2}$ and $^4F_{9/2}$ sates has been measured at $T = 300$ K.

The intensities of the absorption lines of this glass, expressed in terms of oscillator strength f, are analysed with the help of the Judd–Ofelt theory [20, 21]. In this approach, the oscillator strength for an electric-dipole transition between two J states is given by [22]:

$$f_{ij} = \frac{8\pi^2 m\nu}{3h(2J+1)}\chi \sum_{t=2,4,6} \Omega_t |\langle aSL, J|U^{(t)}|aS'L', J'\rangle|^2. \tag{1}$$

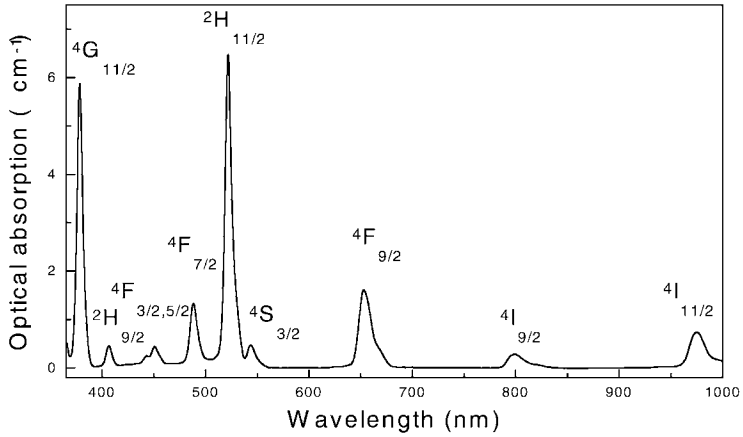

Figure 1. Absorption spectrum of 2 at.% Er^{3+} in $70TeO_2$–30 ZnO glass at room temperature.

Here, ν is the transition frequency, $(2J + 1)$ the ground-state degeneracy and χ the field correction factor, given by: $\chi = (n^2 + 2)^2/9n$ where n is the refractive index of the material whose value is 2.036 [23]. Ω_t are Judd–Ofelt parameters, J and J' represent the total angular momentum of initial and final states, aSL define all other quantum numbers needed to specify the states, and $\langle \ldots |U^{(t)}| \ldots \rangle$ are double reduced matrix elements of unit tensor operators calculated in the intermediate coupling approximation. Because the matrix elements are essentially the same from host to host for a given rare earth ion [24], we have used in this work the values calculated by Weber [25] for Er^{3+} in LaF_3. Experimental values of the oscillator strength, f_{expt}, corresponding to the observed absorption transitions have been computed using the following expression:

$$f_{expt} = \frac{mc}{\pi e^2 N} \int \alpha(\nu)\, \mathrm{d}\nu \tag{2}$$

where m and e are the mass and the charge of the electron, c is the speed of light, $\alpha(\nu)$ is the absorption coefficient at frequency ν, and N is the number of optically active ions per cm^3. A least squares fit of f_{expt} using equation (1) was carried out to determine the Judd–Ofelt parameters. The Ω_t parameters obtained are $\Omega_2 = 5.93 \times 10^{20}$, $\Omega_4 = 1.50 \times 10^{20}$ and $\Omega_6 = 1.07 \times 10^{20}$ cm^2. The root mean square deviation ($\delta_{RMS} = [\sum(\Delta f)^2/(N_{Trans} - N_{Param})^{1/2}$) was found to be 1.82×10^{-6}. It has to be noticed that the values of Ω_4 and Ω_6 agree well with those reported by Reisfeld for Er^{3+} in banary germanate and tellurite glasses [26], whereas our Ω_2 parameter is lower than that in [26], but closer to Ω_2 values reported by Ryba-Romanowski [27] and Pan *et al* [12, 28] for Er^{3+} in tellurite-glasses.

Once the intensity parameters have been determined, the electric dipole radiative probabilities can be estimated using:

$$A_{ij} = \frac{8\pi \nu^2 n^2 e^2}{mc^2} f_{ij}. \tag{3}$$

Additionally, the radiative lifetime of an excited state i, $\tau_r(i) = 1/\sum_j A_{ij}$ and the branching ratio, $\beta_{ij} = A_{ij}/\sum_j A_{ij}$ can be estimated for the main emission channels. The corresponding values of transition probabilities, radiative lifetimes and branching ratios are summarized in table 1. As seen, the luminescence of the Er^{3+} ions predominantly arises from the transitions $^4S_{3/2}$–$^4I_{15/2}$ and $^4F_{9/2}$–$^4I_{15/2}$. The emitting levels $^4S_{3/2}$ and $^4F_{9/2}$ are expected to be most efficient in up-conversion as well. An illustration of this expectation will be given in the following.

Table 1. Radiative transition probabilities, lifetimes, and branching ratios of $^4S_{3/2}$ and $^4F_{9/2}$ excited states of Er^{3+} in $70TeO_2$–30ZnO glass.

Transition	Energy (cm^{-1})	A_{ij} (s^{-1})	B_{ij} (%)	τ_R (μs)
$^4S_{3/2} \rightarrow {}^4 I_{15/2}$	18 085	2333	66.1	
$^4S_{3/2} \rightarrow {}^4 I_{13/2}$	11 780	982	27.8	
$^4S_{3/2} \rightarrow {}^4 I_{11/2}$	8200	80	2.3	283
$^4S_{3/2} \rightarrow {}^4 I_{9/2}$	5950	133	3.8	
$^4F_{9/2} \rightarrow {}^4 I_{15/2}$	15 067	2972	90.2	
$^4F_{9/2} \rightarrow {}^4 I_{13/2}$	8720	165	5.0	304
$^4F_{9/2} \rightarrow {}^4 I_{11/2}$	5070	148	4.5	
$^4F_{9/2} \rightarrow {}^4 I_{9/2}$	2800	8	0.3	

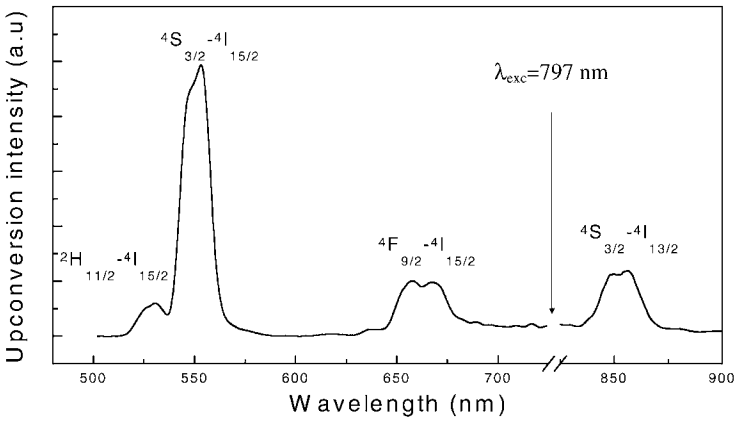

Figure 2. Up-conversion luminescence of 0.4 at.% Er^{3+} in $70TeO_2$–30ZnO glass at $T = 300$ K, $\lambda_{ext} = 797$ nm.

4. Up-conversion results

4.1. Up-conversion luminescence in $70TeO_2$–30ZnO glass: 0.4% Er^{3+}

The up-conversion emission spectrum in the range 500–900 nm for this sample at room temperature pumped with 797 nm line excitation is shown in figure 2. The spectrum exhibits four distinct emission bands. The green luminescence corresponding to the ($^2H_{11/2}$, $^4S_{3/2}$)–$^4I_{15/2}$ transitions of Er^{3+} at 530 and 554 nm can readily be seen by the naked eye for pump powers lower than 100 mW. This observation indicates a considerable efficient up-conversion process in such a host glass. Figure 2 also shows a red emission band centred around 663 nm and a near infrared band (849 nm). The two emission bands are identified as the $^4F_{9/2}$–$^4I_{15/2}$ and $^4S_{3/2}$–$^4I_{13/2}$ transitions, respectively.

The relative intensity of the up-converted emission at 554 nm has been measured versus the pump power at 797 nm. The power dependence of this intensity is plotted in a logarithmic scale, figure 3. It follows from the slope of this plot that the power dependence of the green emission exhibits a gradient of 1.8. This indicates that the $^4S_{3/2}$–$^4I_{15/2}$ emission is a two-step up-conversion process. The energy levels illustrating the up-conversion process under 797 nm excitation are shown in figure 4.

The blue $^2H_{9/2}$–$^4I_{15/2}$ up-conversion transition around 410 nm has been barely observed at room temperature. This shows that a third step excitation is necessary to achieve the $^2H_{9/2}$

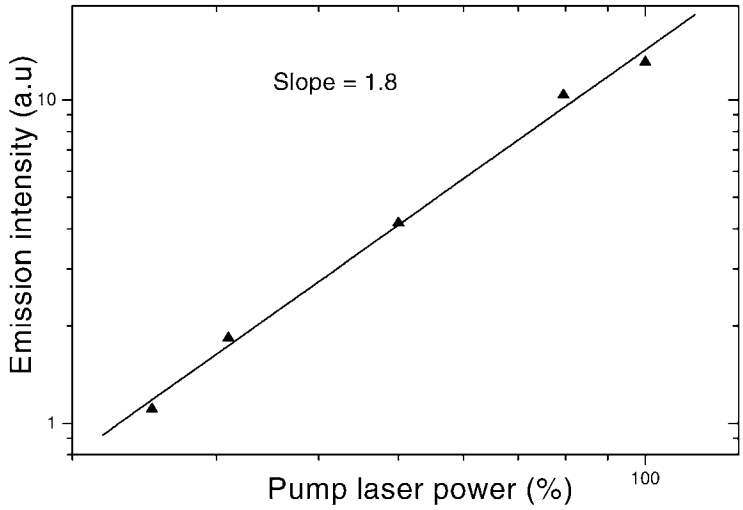

Figure 3. Intensity of the up-converted green emission from Er^{3+} versus power excitation for a 0.4 at.% Er^{3+} in $70TeO_2$–30ZnO glass using a 797 nm excitation. Measurements were performed at 300 K.

emitting level using the 797 nm pump excitation. The energy levels illustrating up-conversion process under 797 nm excitation are shown in figure 4.

4.2. Effects of ion concentration in up-conversion luminescence

Figure 5 shows up-conversion luminescence spectra obtained in Er^{3+}-doped tellurite glass at room temperature for different concentrations ranging from 0.2 to 4 mol.% Er_2O_3 under the 797 nm excitation line. The intensities of up-conversion emissions have been normalized relative to the green band. Two main features are observed: (i) for a low content of Er^{3+} (0.4 at.%) the dominant emission is in the green corresponding to the $^4S_{3/2}$–$^4I_{15/2}$ transition, (ii) when the Er^{3+} concentration increases, the green emission enhances, and the red transition shows a rapid growth relative to the green up-converted line (figure 5). Basically, there are two up-conversion processes, excited-state absorption (ESA) and energy-transfer up-conversion (ETU) [1, 3]. In the case of higher Er^{3+} concentrations, both ESA and ETU are active. In the ETU process, energy migrates from a donor to an acceptor in an isolated ion pair and/or in a cluster, raising the latter ion into a higher energy excited state. For a given system of RE ions in a host lattice, different excited-state dynamics can participate in energy migration [29]. With the up-converted transition of $^4S_{3/2}$–$^4I_{15/2}$ being observed in the 0.4 at.% Er^{3+} doped glass, this shows that the green emission mainly originates from the first mechanism which is assisted by multiphonon relaxations. This assignment is supported by the fact that energy-transfer between excited ions can be ignored for a single concentration lower than 0.5 at.% [30]. We will give for the system studied a possible ETU process between an ion-pair (A, B) with one in the excited $^4I_{9/2}$ level and another in the ground state $^4I_{15/2}$ and which contributes to the enhancement of this emission. This energy transfer is assumed to be produced according to the reaction (see figure 6(a)):

$$^4I_{9/2}(A) + {}^4I_{15/2}(B) \rightarrow {}^4I_{13/2}(A) + {}^4I_{13/2}(B) \tag{4}$$

By absorption of 797 nm pump photons, $^4I_{13/2}$–$^2H_{11/2}$ transitions can indeed occur, leading to an increase in the $^4S_{3/2}$–$^4I_{15/2}$ up-converted emission. For lower Er^{3+} concentrations, the

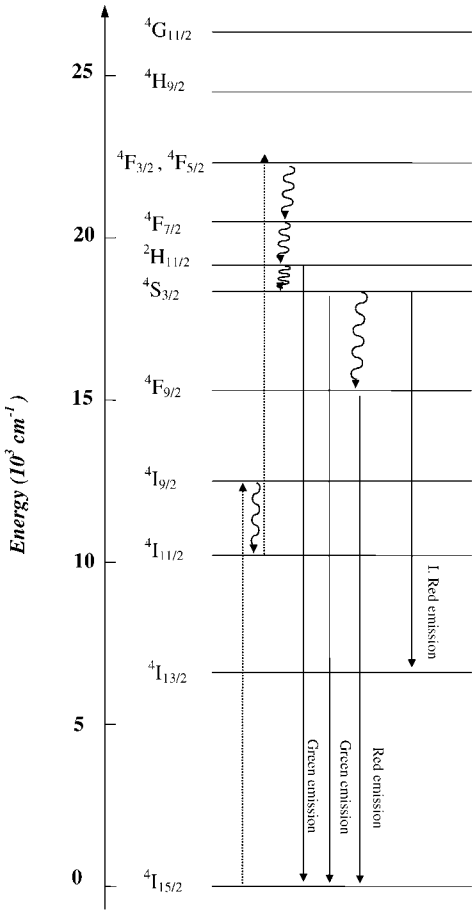

Figure 4. Energy-level diagram for a two-step infrared to visible up-conversion of Er^{3+} in $70TeO_2$–30ZnO glass under 797 nm excitation. The dashed lines indicate up-conversion pumping, solid lines indicate radiative transitions and waved lines show nonradiative decay.

$^4F_{9/2}$ level can possibly be populated via a non-radiative relaxation through the $^4S_{3/2}$ excited state with a moderate rate [31]. Thus, the increase in the red up-converted line with increased Er^{3+} concentration must therefore result from an energy transfer between excited ions. A possible scheme which can explain the behaviour of this emission is a subsequent energy transfer cross-relaxation from a state in which one Er^{3+} ion is in $^4I_{9/2}$ and another in $^4S_{3/2}$ leads to two ions in the intermediate $^4F_{9/2}$ level, as illustrated in figure 6(b). This mechanism has been proposed by Pan *et al* [31] to explain the trend of this transition in Er^{3+}-doped lead–germanate glass. The authors found that the intensity of the red emission in this glass system is only $\leqslant 5\%$ of the total emitted light. This indicates that the quenching of the Er^{3+} ions from the $^4S_{3/2}$ level does not significantly reduce the intensity of the green up-converted emission. Our results, however, show that the red emission accounts for more than 10% of the up-conversion intensity in the glass doped with 0.4 at.% Er^{3+}. Furthermore, this transition exceeds the green up-converted line for higher Er^{3+} concentrations (>6.0 at.%). The ETU process, shown in figure 6(b), favours the up-conversion from the emitting level $^4F_{9/2}$. This process, however, reduces the efficiency of the $^4S_{3/2}$–$^4I_{15/2}$ transition. This can explain in part

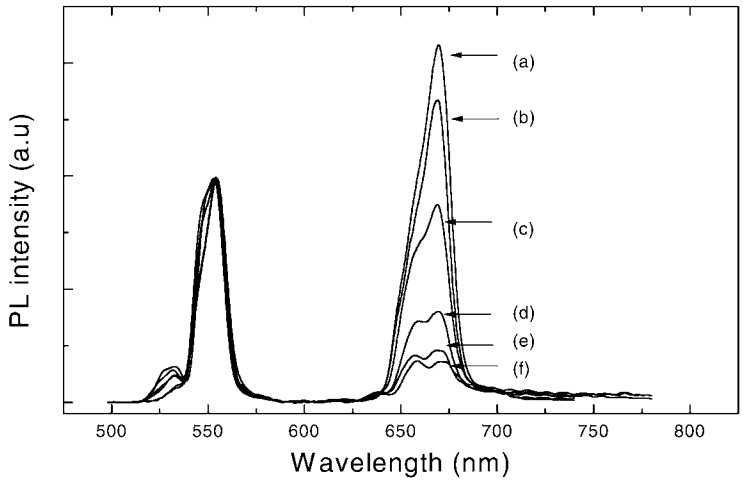

Figure 5. Up-conversion luminescence spectra of Er^{3+}-doped zinc–tellurite glasses with different Er_2O_3 concentrations: (a) 4.0 mol.%, (b) 3.0 mol.%, (c) 2.0 mol.%, (d) 1.0 mol.%, (e) 0.5 mol.% and (f) 0.2 mol.% excited by 797 nm laser line. The intensities of emission are normalized to the green up-conversion band (554 nm).

the behaviour of the red emission. On the other hand, when the content of the Er^{3+} increases, non-radiative processes can take place, leading to the depopulation of the $^4S_{3/2}$ level. Such processes could be non-radiative energy transfer from Er^{3+} ions to unintentionally introduced impurities and/or structural defects. Evidence of the latter process has been given by the study of the Er^{3+} concentration effects on the PL intensity. Indeed, we have observed that the PL transition of $^4F_{9/2}$–$^4I_{15/2}$ increases with increased Er^{3+} concentration relative to the PL transition $^4S_{3/2}$–$^4I_{15/2}$. It should be noticed that the PL red emission does not exceed the green one in the range of Er^{3+} concentrations studied.

4.3. Temperature-dependent up-conversion

In the previous section, we have studied the effects of the Er^{3+} concentration on both up-converted $^4S_{3/2}$–$^4I_{15/2}$ and $^4F_{9/2}$–$^4I_{15/2}$ transitions. The potentially interesting observation of this study was the enhancement of the up-conversion efficiency with increased Er^{3+} concentration. This behaviour has been explained as due to an energy transfer between RE ions. This does not, however, exclude the presence of competitive processes, which tend to quench the up-conversion luminescence. As evidence for this proposal, a decay in luminescence in a tellurite glass with Er^{3+} concentration and temperature has also been observed by Ryba-Romanowski [27]. Such a quenching has been assigned to a non-radiative energy transfer between active ion-pairs. An energy transfer from Er^{3+} ions to unintentionally introduced impurities and/or structural defects has been also evoked to be possibly at the origin of this quenching. The author has analysed quantitatively the quenching by computing the rate $1/\tau_m - 1/\tau_0$ where is the measured luminescence lifetime and τ_0 is the lifetime calculated taking into account the radiative recombination and multiphonon relaxation rates. The temperature dependence of the luminescence showed an exponential behaviour at high temperature that is characterized by an activation energy. For the transitions $^4S_{3/2}$–$^4I_{15/2}$ and $^4I_{11/2}$-$^4I_{15/2}$, the relevant activation energies are 58 and 210 meV, respectively. However, no assignment has been proposed for these activation energies. Tanabe *et al* [9] have studied, on the other hand,

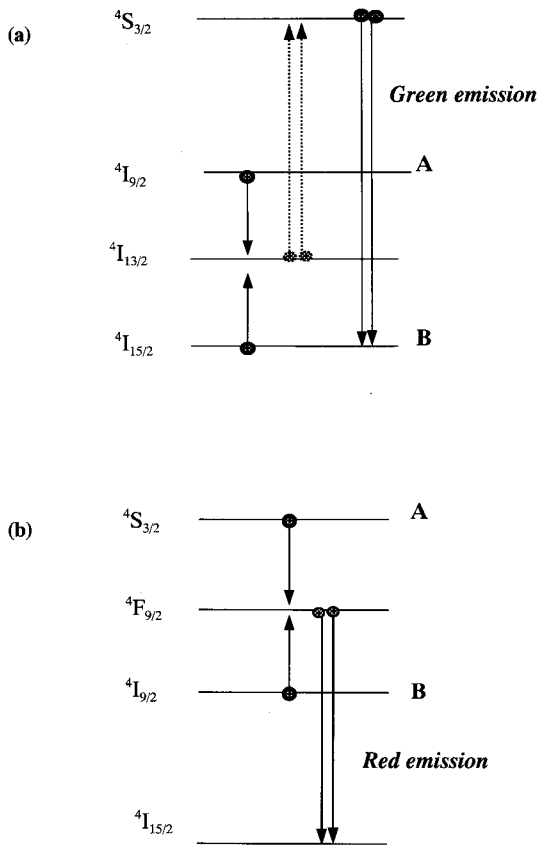

Figure 6. Schematic representation of the ETU processes for (a) $^4S_{3/2}$–$^4I_{15/2}$ emission and (b) $^4F_{9/2}$–$^4I_{15/2}$ up-converted transition.

the temperature dependence of up-conversion intensity between 300 and 650 K in fluoride and fluorophosphate glasses. The authors observed a thermal quenching of the $^4S_{3/2}$–$^4I_{15/2}$ emission. They have examined the effects of glass composition on the behaviour of this quenching. It is concluded that the efficiency of the up-conversion process is mainly governed by the lifetime of the intermediate level $^4I_{11/2}$ which is influenced by the phonon mode locally coupled to the RE ion in the glass. Ourselves, we have studied the effects of temperature on the up-conversion processes in a tellurite glass system $70TeO_2$–30ZnO doped with 1 at.% Er^{3+}. The temperature range investigated extends from 40 to 310 K. Figure 7 shows the temperature dependence of the up-conversion intensity of both $^4S_{3/2}$–$^4I_{15/2}$ and $^4F_{9/2}$–$^4I_{15/2}$ emissions. The intensity of the $^4S_{3/2}$–$^4I_{15/2}$ transition decreases by about 1/5 as the temperature increases from 100 to 310 K. The red emission, however, does not show a significant thermal quenching in the temperature range 40–310 K studied. Theoretically, this quenching has usually been analysed by taking into account the multiphonon relaxation process [32]. Accordingly, the fact that the red up-converted line quenches smoothly compared with the green emission $^4S_{3/2}$–$^4I_{15/2}$ means that the multiphonon relaxation channel mainly affects the emitting level $^4S_{3/2}$. Assuming that the thermal quenching of up-conversion is induced only by the multiphonon relaxation process, the decay rate can be expressed as the sum of the radiative and multiphonon

relaxation rates W_r and W_p [18, 32] as follows:

$$W = W_r + W_p \tag{5}$$

with

$$W_p(T) = C_P \exp(-\alpha \Delta E)\left[1 - \exp\left(-\frac{\hbar\omega}{K_B T}\right)\right]^{-p}$$

where C_P and α are non-radiative parameters which depend on the host material, ΔE represents the energy gap between two successive levels and $p = \frac{\Delta E}{\hbar\omega}$ is the number of phonons emitted in the relaxation process. According to this assumption, the expected temperature dependence of the up-conversion intensity can be written for an emitting level as:

$$\eta = \frac{W_r}{W_r + W_p}. \tag{6}$$

In the case of the $^4S_{3/2}$–$^4I_{15/2}$ transition we have calculated the quantum efficiency using equation (6) in the temperature range 40–350 K with $W_r = 3528\ s^{-1}$, $\Delta E = 3000\ cm^{-1}$, $\alpha = 4.7 \times 10^{-3}$ cm, and $\hbar\omega = 750\ cm^{-1}$. The results are summarized in figure 8 (dashed line). As clearly seen, a best fit can be obtained at a low temperature for the parameter $C_P = 6.3 \times 10^9\ s^{-1}$. However, this equation can not account for the experimental data in the high temperature range. Further, taking into account the multiphonon relaxation rate of the intermediate level $^4I_{11/2}$, no appreciable change has been observed in the trend of the quantum efficiency, particularly at high temperature limit. Following Ryba-Romanowski [27] we have written the total decay rate in the form:

$$W = W_r + W_p + W_t \tag{7}$$

where W_t is the decay rate describing processes, other the radiative and the multiphonon relaxation mechanisms, which could be at the origin of the thermal quenching of up-conversion. To express the rate W_t, we have adopted the experimental low obtained from the variation of the PL intensity versus temperature:

$$W_t = C_T \exp\left(-\frac{E_\Delta}{K_B T}\right) \tag{8}$$

where E_Δ represents the activation energy and C_T is a constant, treated as a fitting parameter. Using the latter expression for W_t, the quantum efficiency of up-conversion will be given by:

$$\eta = \frac{1}{1 + W_p/W_r + C_T/W_r \exp(-E_\Delta/K_B T)}. \tag{9}$$

In figure 8 we show the intensity variation of the $^4S_{3/2}$–$^4I_{15/2}$ transition in the sample doped with 1 at.% Er^{3+}. From the slope of this plot at high temperature we have deduced an energy activation E_Δ of the order 59 meV, assuming that the intensity decreases exponentially in this temperature range. For this value of the activation energy E_Δ, we have computed the quantum efficiency η from equation (9), figure 8 (in solid line). As can be seen, a good agreement between experimental and theoretical results has been obtained in the temperature region investigated for the parameters $C_P = 6.3 \times 10^9\ s^{-1}$ and $C_T = 1.3 \times 10^5\ s^{-1}$. Using this approach, we have analysed, the temperature-dependent up-conversion results obtained by Tanabe *et al* [9] for the transition $^4S_{3/2}$–$^4I_{15/2}$ in fluoride and fluorophosphate glasses (see the inset of figure 8). As shown, the variation of up-conversion intensity is exponential. The relevant thermal energies from these plots are 115 and 35 meV, respectively. As well demonstrated from this study: (i) the multiphonon relaxation process alone is unable to explain the thermal quenching of the $^4S_{3/2}$–$^4I_{15/2}$ transition, (ii) the fit of experimental data

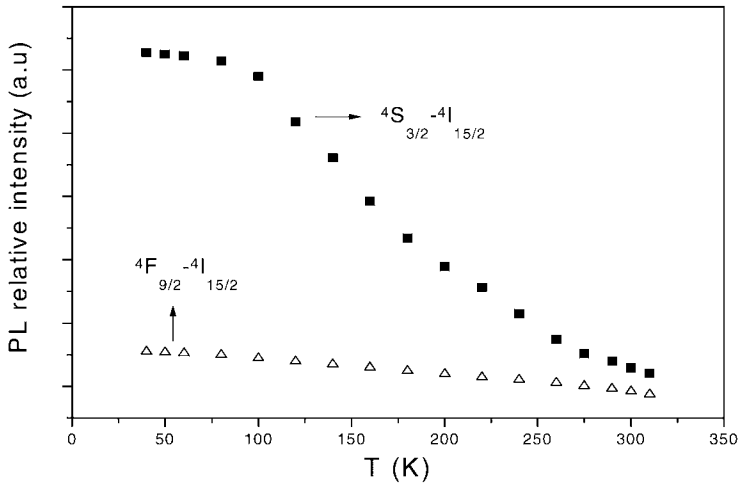

Figure 7. Temperature dependence of up-conversion intensity for both $^4S_{3/2}$–$^4I_{15/2}$ (■) and $^4F_{9/2}$–$^4I_{15/2}$ (△) transitions in zinc-tellurite glass.

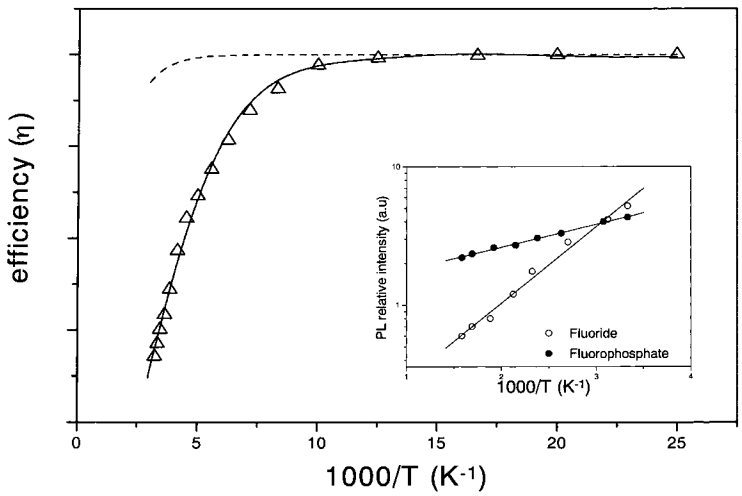

Figure 8. Variation of the relative intensity $I(T)/I(T = 40\ \mathrm{K})$ for the up-converted transition $^4S_{3/2}$–$^4I_{15/2}$ transition versus temperature in 1 at.% Er^{3+}-doped tellurite glass. The dashed and solid lines represent the quantum efficiencies calculated from equations (6) and (9), respectively. The inset shows the variation of up-conversion intensity of this emission in fluoride (○) and fluorophosphate (●) glasses taken from [9].

has been made possible by adding to W_r and W_p a rate W_t which involves a thermal energy, (iii) the activation energy is larger in fluoride glass than in tellurite and fluorophosphate. Therefore, the non-radiative transition rate W_t decreasing in the sequence fluoride < tellurite < fluorophosphate results in agreement with those reported in the literature [18]. The origin of such thermal quenching is not clear. One possible explanation is a phonon assisted cross relaxation via an intermediate level or an energy transfer to unintentionally introduced impurities and/or structural defects. Another possibility is to assign this thermal quenching to a charge transfer through trapping impurities. Unlike the $^4S_{3/2}$–$^4I_{15/2}$ transition, the red

emission $^4F_{9/2}$–$^4I_{15/2}$ is not affected appreciably by these processes. This behaviour can be understood as due possibly to a large activation energy E_Δ for the $^4F_{9/2}$ level. The fact that this emission is smoothly sensitive to temperature and its intensity increases drastically with increasing Er^{3+} concentration can make this transition promising in technological applications.

We have also studied the temperature dependence of the $^2H_{11/2}$–$^4I_{15/2}$ transition. We have observed that the intensity of this line increases with increasing temperature. This behaviour is similar to that previously reported in [15] and which has been explained as due to a thermal population of the $^2H_{11/2}$ level through the $^4S_{3/2}$ one.

5. Conclusion

Absorption and photoluminescence measurements were performed on Er^{3+}-doped $70TeO_2$–30ZnO glasses. The Judd–Ofelt intensity parameters and radiative transition rates have been calculated. We have also investigated the room temperature infrared to visible up-conversion of Er^{3+} in this host with different concentrations ranging from 0.2 to 4 mol.% Er_2O_3, excited by a 797 nm excitation line. The green emission corresponding to the $^4S_{3/2}$–$^4I_{15/2}$ transition of Er^{3+} is dominant at low concentration in the spectral region studied (20 000–11 100 cm^{-1}). The red emission $^4F_{9/2}$–$^4I_{15/2}$ is enhanced considerably relative to the green up-converted transition with increased Er^{3+} concentration. This behaviour has been explained as due to an ETU process. The study of temperature-dependent up-conversion intensity has been performed in the sample containing 1 at.% Er^{3+} in the range 40–310 K. It was found that the thermal quenching of the green emission is large compared with those of the red transition. This thermal quenching has been analysed in terms of multiphonon relaxation and by adding a non-radiative transition rate. The origin of the latter rate could be presumably an energy transfer from Er^{3+} ions to energy sinks or a charge transfer through trapping impurities.

References

[1] Auzel F 1973 *Proc. IEEE* **61** 758
[2] Watts R K 1974 Optical properties of ions in solids *(Nato Advanced Study Institutes Series)* vol 8, ed B Di Bartolo (New York: Plenum) p 337
[3] Wright J C 1976 Radiation processes in molecules and condensed phases *(Topics in Applied Physics)* vol 15, ed F K Fong (New York: Springer) p 239
[4] Reddy B R and Venkateswarlu P 1994 *Appl. Phys. Lett.* **64** 1327
[5] Pollak S A, Chang D B and Moise N L 1986 *J. Appl. Phys.* **60** 4077
[6] Auzel F 1990 *J. Lumin.* **45** 341
[7] Amorim H T, Araugo M T, Gouveia E A, Gouveia-Neto A S, Neto J A M and Somora A S B 1998 *J. Lumin.* **78** 271
[8] Reddy B R and Nash-Stevenson S K 1994 *J. Appl. Phys.* **76** 3896
[9] Tanabe S, Yoshii S, Hirao K and Soga N 1992 *Phys. Rev.* B **45** 4620
[10] Yeh D C, Sibley W A, Schneider I, Afzal R S and Aggarwal I 1991 *J. Appl. Phys.* **69** 1648
[11] Silversmith A J, Lenth W and Macfarlane R M 1987 *J. Appl. Phys.* **51** 1977
[12] Pan Z, Morgan S H, Dyer K, Ueda A and Liu H 1996 *J. Appl. Phys.* **79** 8906
[13] Jacob R R and Weber M J 1976 *IEEE Trans. Quantum Electron.* **12** 102
[14] Weber M J 1967 *Phys. Rev.* B **157** 262
[15] Shin M D, Sibley W A, Drexhage M G and Brown R N 1983 *Phys. Rev.* B **27** 6635
[16] Chamarro M A and Cases R 1990 *J. Lumin.* **46** 59
[17] Kumar V R, Veeraiah N and Rao B A 1997 *J. Lumin.* **75** 57
[18] Wang J S, Vogel E M and Snitzer E 1994 *Opt. Mater.* **3** 187
[19] Tanabe S, Hirao K and Soga N 1990 *J. Non-Cryst. Solids* **122** 79
[20] Judd B R 1962 *Phys. Rev.* **127** 750
[21] Ofelt G S 1962 *J. Chem. Phys.* **37** 511
[22] Weber M J, Myers J D and Blackburn D H 1981 *J. Appl. Phys.* **52** 2944

[23] Redman M J and Chem J H 1967 *J. Am. Ceram. Soc*. **50** 523
[24] Lakshman S V J and Ratnakaram Y C 1988 *J. Non-Cryst. Solids* **101** 75
[25] Weber M J 1967 *Phys. Rev.* **157** 262
[26] Reisfeld R 1973 *Structure and Bondings* vol 13 (New York: Springer) p 136
[27] Ryba-Romanowski W 1990 *J. Lumin.* **46** 163
[28] Pan Z and Morgan S H 1997 *J. Lumin.* **75** 301
[29] Hehlen M P, Frei G and Gûdel H U 1994 *Phys. Rev.* B **50** 16 265
[30] van der Ziel J P, Van Uitert L G, Grodkiewicz W H and Mikulyak R M 1986 *J. Appl. Phys.* **60** 4262
[31] Pan Z, Morgan S H, Loper A, King V, Long B H and Collins W E 1995 *J. Appl. Phys.* **77** 4688
[32] Riseberg L A and Moos H W 1968 *Phys. Rev.* **174** 429